How to cite: *Angew. Chem. Int. Ed.* **2022,** *61,* e202115026
International Edition: doi.org/10.1002/anie.202115026
German Edition: doi.org/10.1002/ange.202115026

Radical Cage Species

Isolation and Properties of the Long Elusive Deep Blue Soluble $[K_3\{(N^tBu)_3S\}_2]^\bullet$ Cage Radical

*Christina M. Legendre, A. Claudia Stückl, Christian P. Sindlinger, Regine Herbst-Irmer, and Dietmar Stalke**

Dedicated to Professor Holger Braunschweig on the occasion of his 60th birthday

Abstract: *The reaction of potassium metal with sulfurtriimide $S(N^tBu)_3$ (**II**) gives the long elusive deep blue cage radical $[K_3\{(N^tBu)_3S\}_2]^\bullet$ (**1_K**) that crystallizes at −35 °C from toluene solution. The subsequent physical characterization via X-ray structure analysis, UV/Vis-, and EPR spectroscopy from solution reveals the existence of one unpaired electron delocalized within the whole cage, i.e. coupling with the six nitrogen atoms, as well as the three potassium atoms caped by the two SN_3 ligands. The present X-ray structure analysis further supports previous assumptions made on the parent compound **1_Li** obtained from $[Li_4\{(N^tBu)_3S\}_2]$ (**I**) and finally elucidates the structural arrangement of the SN_3 caps and alkali metals in such radical cage species.*

Radicals containing main group elements offer rich and versatile platforms towards synthetically challenging compounds with various applications.[1] Their fascinating colors and chemistry gave birth to numerous investigations.[2] Notably, intense-colored persistent radicals were obtained from alkali metal derivatives of polyimido anions with p-block elements.[3–7] These include our contribution with the EPR study of the deep blue lithium-based radical species $[Li_3\{(N^tBu)_3S^{IV}\}_2]^\bullet$ (**1_Li**), as the resulting oxidation product of the cage complex $[Li_4\{(N^tBu)_3S^{IV}\}_2]$ (**I**) (Scheme 1).[3,8] Its crystal structure, however, could never be reported due to the high reactivity of transient **1_Li**, and attempts to isolate **1_Li** systematically led to the characterization of fully oxidized products. Several other works focused on the elucidation of similar radical species, such as $[\{Li_nE(N^tBu)_3\}_2]^\bullet$, $n=2, 3$; E = B,[9] S,[3,6,8] Se[6,10]) and $[Me_3SiNP(\mu_3\text{-}N^tBu)_3\{\mu_3\text{-}Li(thf)\}_3X]^\bullet$, (X = Br, I).[5,11] Most of the solid-state structures of these compounds, however, could not be determined until now, because of the high sensitivity of the radical species.[3] Hypotheses about the potential molecular arrangements were postulated based on the analysis of the EPR spectra in solution.[3,6,8,9] While seeking for heavier alkali metal derivatives to enhance the radical species' stability, we were able to synthesize, isolate and characterize the long sought-after radical species $[K_3\{(N^tBu)_3S\}_2]^\bullet$ (**1_K**), which is analogous to **1_Li**. We herein report its solid-state structure as well as its physical characterization via UV/Vis and EPR spectroscopies. Experimental features are also backed-up by computational chemistry.

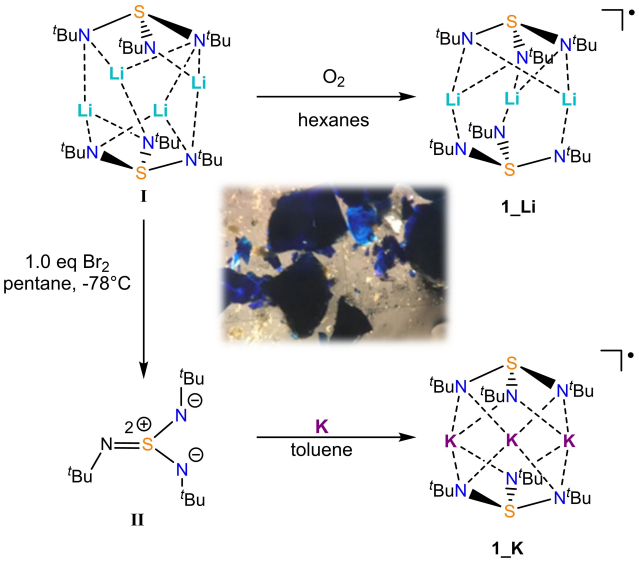

Scheme 1. Synthetic route to the radical species **1_K**. The structure of the analogous **1_Li** compound is proposed based on EPR results reported elsewhere.[3] Picture of the deep blue crystals (center).

The elusive deep blue radical $[K_3\{(N^tBu)_3S\}_2]^\bullet$ (**1_K**) can be obtained from neutral, colorless $S^{VI}(N^tBu)_3$ (**II**) upon the addition of ultrapure potassium metal in toluene (Scheme 1). Subsequent to filtration, the deep blue solution is reduced in volume for crystallization. Highly unstable, the solid-state samples and solutions of **1_K** must be stored at low temperatures all the time.

Crystals suitable for X-ray structure analysis can be grown at −35 °C from a toluene solution (Scheme 1). The structure is shown in Figure 1.[12] At 120 K, **1_K** exists in the monoclinic space group $P2_1/c$. A further data set from a different crystal at 100 K resulted in a structure solution in

[*] Dr. C. M. Legendre, Dr. A. C. Stückl, Prof. Dr. C. P. Sindlinger, Dr. R. Herbst-Irmer, Prof. Dr. D. Stalke
Georg-August Universität Göttingen
Institut für Anorganische Chemie
Tammannstraße 4, 37077 Göttingen (Germany)
E-mail: dstalke@chemie.uni-goettingen.de

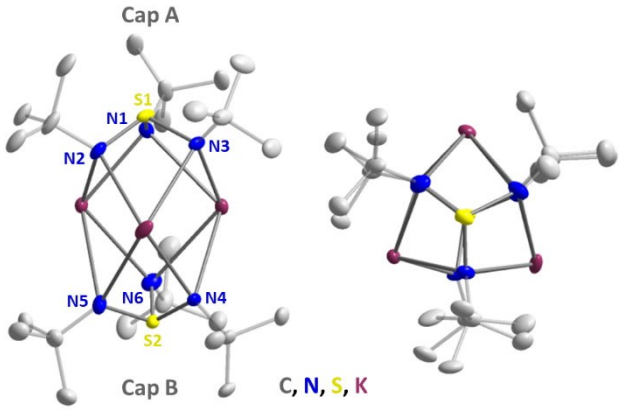

Figure 1. Crystal structure of **1_K** in side view (left) and top view (right). Hydrogen atoms are omitted for clarity. Anisotropic displacement parameters are depicted at the 50% probability level. Selected bond lengths [Å]: **Cap A**: S1–N1 1.608(3), S1–N2 1.610(3), S1–N3 1.676(3); **Cap B**: S2–N4 1.643(3), S2–N5 1.642(3), S2–N6 1.647(3). Bond lengths and angles for **1_K** at 100 K are reported in the Supporting Information.

$P2_1/c$ with the doubled cell volume and two crystallographically independent molecules in the asymmetric unit (see Supporting Information section S2 for more details). No phase transition was observed by varying the temperature directly on the diffractometer, which suggests close lattice energies for these two polymorphs. Generally, both structures show the same features. All molecules display three equilateral triangular arranged potassium atoms caped by a formally radical monoanionic $S(N^tBu)_3^{\bullet-}$ and a dianionic $S(N^tBu)_3^{2-}$ ligand in a tripodal ecliptic fashion. This trigonal-pyramidal structure is known from the isosteric AsS_3^{3-} trianion in Li_3AsS_3.[13] Every metal is *N*,*N*′-chelated by two nitrogen atoms of both caps each. Hence, each potassium atom is coordinated by four nitrogen atoms to give a square-pyramidal polyhedron. The K–N bond lengths cover a wide range of av. 2.62 to 3.02 Å. Interestingly, at 120 K, the upper capping ligand **Cap A** shows one much longer S–N bond, while the two remaining are shorter and of the same length (1.676(3) vs. 1.608(3) and 1.610(3) Å), whereas at 100 K there is also one longer S–N bond lengths and two shorter in **Cap A**, but the differences are much smaller and the longer bond length is similar to those in **Cap B**. The lower **Cap B** displays three equivalent S–N bond lengths (1.643(3), 1.642(3) and 1.647(3) Å) in both structures. The bond length situation in solid **1_K** might mirror those in the *N*,*N*′-chelated complex $[Cp^*_2Ln\{(NSiMe_3)_2S\}]$,[4] in which the S–N bond lengths in the monoanionic radical $[S(NSiMe_3)_2]^{\bullet-}$ sulfurdiimide ligand are elongated by ca. 0.10 Å compared with the free ligand,[14] consistent with the occupation of the π* SOMO of the radical anion. Additionally, all the S–N distances in **1_K** are significantly longer than those found in similar S^{VI} compounds[15] (S–N distances of 1.53–1.60 Å) and comparable to those of similar S^{IV} compounds.[16] This is indicative of the sulfur atoms in **1_K** holding the oxidation state +IV, reminiscent of pyramidal sulfite SO_3^{2-} and not of trigonal-planar SO_3. Hence, the pyramidal cap-shaped structure is due to a stereochemically active lone-pair at the central sulfur atom each, experimentally determined previously,[17] or rather the unpaired electron (see a schematic overview in Figure S4.4.1).

While the disorder of the substituents in the crystal structure prevents experimental charge density investigations, the subsequent physical characterization of the crystalline powder confirms the presence of a radical species. Since diluted solutions of **1_K** lose color intensity over time, which may be due to potassium ions solvation[11] and/or to radical instability in solution, UV/Vis and EPR spectroscopic experiments are quite challenging and must be performed instantaneously on freshly prepared diluted cold solutions. The UV/Vis spectrum of **1_K** in toluene (Figure 2) reveals a broad unstructured absorption band from approx. 750 to 550 nm with a maximum at 635 nm. An additional small shoulder is detectable around 400 nm. TD-DFT calculations at the CAM B3LYP/def2-TZVP level of theory, predict a similar absorption pattern (Figures S4.1.1, S4.2.1 with similar band broadening). Furthermore, both experimental and theoretical results are very similar to those of the reference lapis lazuli (from the lazurite pigment) containing the trisulfur radical anion $S_3^{\bullet-}$[18] (601 nm) or Egyptian blue (630 nm).[19]

We further performed a time-dependent UV/Vis measurement of $[Li_4\{(N^tBu)_3S^{IV}\}_2]$ (**I**) upon exposure to air to monitor the formation of **1_Li** from **I**. It is clear that **1_Li** forms, as a strong absorption band at 635 nm appears after 2 min, and then decomposes with further exposure to air and moisture to give mainly colorless $[Li_2(N^tBu)_3S^{IV}O]$ and $O_2S^{VI}(^tBuNH)_2$[3] (Figure 3).

Noteworthy, the absorption peak structure around 635 nm is similar in both, wavelength and shape, to that of **1_K** (Figures 2 and 3, S4.1.1 and S4.2.1), which suggests the presence of a blueprint for this radical family in visible spectroscopy. The time-dependency plot (Figure 3, bottom) confirms the instability of compound **1_Li**, which survives about ten minutes on air exposure.

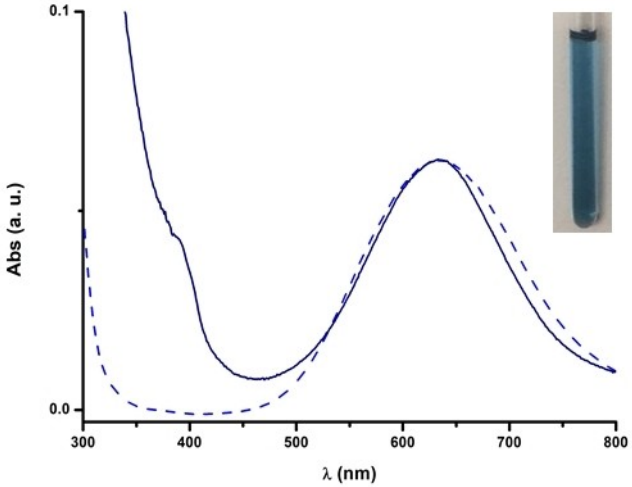

Figure 2. UV/Vis spectrum of **1_K** (dark blue) and **1_Li** (dashed line) in toluene at RT. Photo of a diluted sample of **1_K** in toluene.

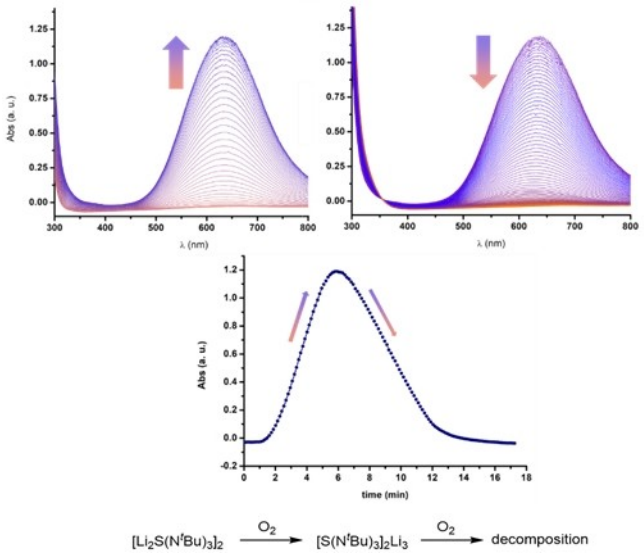

Figure 3. Time-dependent UV/Vis spectra of $[Li_4\{(N^tBu)_3\,S^{IV}\}_2]$ (**I**) upon exposure to air and moisture (formation of **1_Li** (left) and subsequent decomposition (right)), in toluene, at RT. The time dependency of the absorbance at 635 nm is shown below.

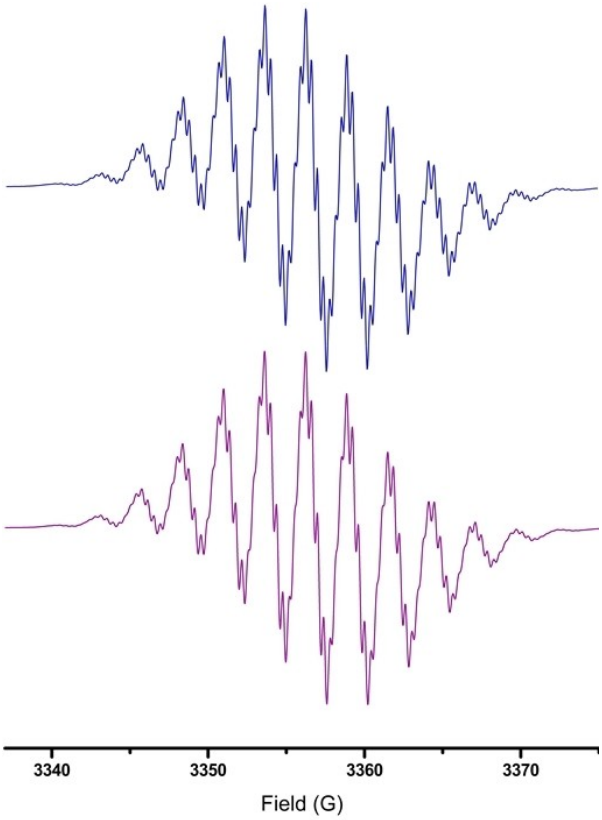

Figure 4. EPR spectrum of **1_K** in toluene at room temperature (top). The simulated spectrum is shown below in purple.

The subsequent EPR investigation of **1_K** in toluene indicates the presence of an unpaired electron, with a symmetrical spectrum as shown in Figure 4, top. In solution at room temperature, the analysis of the hyperfine coupling reveals that the unpaired electron ($g=2.0067$) couples with the six ^{14}N nuclei ($I=1$), resulting in 13 main lines ($m=2I\times 6+1=13$), with an intensity ratio of 1:6:21:50:90:126:141:126:90:50:21:6:1, and a hyperfine constant $a=2.618$ G. Additionally, a super hyperfine coupling is visible in the spectrum, as each of the 13 main lines consists of seven lines with $a\approx 0.379$ G. Coupling with the three central $^{39}K/^{41}K$ nuclei or with the two sulfur ^{33}S nuclei (all possessing a nuclear spin of $I=3/2$) should result in 10 lines ($m=2I\times 3+1=10$) or 7 lines ($m=2I\times 2+1=7$), respectively. Seven of these lines are observable in the EPR spectrum (Figure 4, top).

While the resolution of the experimental spectrum is not entirely complete, it matches well with the simulated spectrum, generated for a hyperfine coupling with the six nitrogen and the three potassium nuclei (Figure 4, bottom). No satisfying simulation was obtained with the sulfur nuclei. Due to the low abundance of ^{33}S (<1%) compared to $^{39}K/^{41}K$ (together ≈100%) and the similarity with the experimental EPR spectrum of **1_Li**, we suggest that the coupling with the potassium nuclei is more reasonable, while the spectral resolution prevents the observation of all 10 lines. Indeed, in comparison, the analogous species **1_Li** gives an EPR spectrum indicating the coupling of the electron with only one hemisphere of the complex: three nitrogen nuclei and the three central lithium atoms are responsible for the hyperfine coupling.[3] This difference from Li to K is most probably due to their different ionic radii and polarizability. While the smaller size of the lithium atoms results in crystallographic disorder over four positions, as observed in oxidation products of **1_Li**, the larger potassium atoms occupy three crystallographically well defined positions, with the nitrogen atoms in an eclipsed conformation (Figure 1). Thus, the electron delocalization is ensured in **1_K**, whereas the symmetry breaking in **1_Li** prevents the electron transit from one SN_3 cap to the other.

Our initial calculations based on the coordinates obtained from X-ray diffraction without further optimization, at the PBE0 D3BJ/def2-tzvp level of theory, suggested that only three nitrogen atoms at the same cap should be involved in electronic coupling (see S4.1 and 4.3, calculations **1_K** UNSYMM for details), as the spin density is localized only on one cap. In line with the experimental EPR spectrum we obtained, which indicates involvement of all 6 nitrogen atoms, we performed subsequent theoretical calculations at the same level of theory on a structure optimized to maintain approximate C_{3h} symmetry (see S4.2 and 4.3 calculation SYMM for more details). The resulting calculations show the spin density to be delocalized on all six nitrogen atoms, which is in better agreement with the EPR spectrum (Figures 5, S4.3.2). The different results of the Mulliken spin population analysis for **1_K** UNSYMM and SYMM well mirror these findings (see S4.3). Additionally, however, it also suggests that the sulfur atoms carry some spin density as well, while the potassium atoms do not. This could indicate that the super hyperfine coupling actually

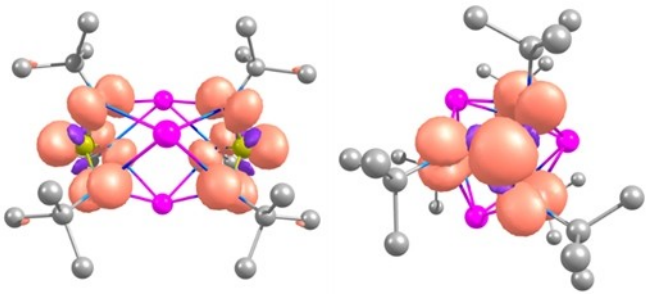

Figure 5. Calculated spin density plots for the symmetry-constrained **1_K** (isosurfaces represented at the 0.005 a.u. level).

occurs with the sulfur nuclei instead of potassium. However, as previously mentioned, we were unable to generate a satisfying simulated EPR spectrum based on this hypothesis and the low abundance of ^{33}S should preclude this possibility. Additionally, given the results observed for **1_Li**, it is unlikely that the free electron would not couple with the alkali metals in both **1_Li** and **1_K**.

In summary, we thoroughly characterized the deep blue radical species **1_K** with a bouquet of physical techniques, as well as by theory. The free electron was discovered to be mainly localized on the nitrogen atoms. The presence of these features was further acknowledged in its parent radical **1_Li** via time dependent UV/Vis spectroscopy. This is a rare report of a long elusive, yet finally captured polyimido radical, which represents a highly important milestone towards further developments of p-block elements containing radical species.

X-ray diffraction data for **1_K** can be found in reference [20].

Acknowledgements

D.S. is grateful for funding from the DFG (STA 334/28-1). C.M.L. acknowledges the Fonds der Chemischen Industrie for financial support (PhD fellowship). Open Access funding enabled and organized by Projekt DEAL.

Conflict of Interest

The authors declare no conflict of interest.

Data Availability Statement

The data that support the findings of this study are available from the corresponding author upon reasonable request.

Keywords: Alkali Metals · EPR Spectroscopy · Radicals · Sulfur–Nitrogen Bonds

[1] a) T. Chivers, R. S. Laitinen, *Chalcogen-nitrogen chemistry, from fundamentals to applications in biological, physical and material sciences*, World Scientific, Singapore, **2021**; b) G. E. Cutsail, *Dalton Trans.* **2020**, *49*, 12128; c) R. Hicks, *Stable Radicals. Fundamentals and Applied Aspects of Odd-Electron Compounds*, Wiley, Chichester, **2010**; d) J. Konu, T. Chivers in *Stable radicals. Fundamentals and applied aspects of odd-electron compounds* (Ed.: R. G. Hicks), Wiley-Blackwell, Oxford, **2010**; e) P. P. Power, *Chem. Rev.* **2003**, *103*, 789.

[2] a) S. Sinhababu, S. Kundu, M. M. Siddiqui, A. N. Paesch, R. Herbst-Irmer, B. Schwederski, P. Saha, L. Zhao, G. Frenking, W. Kaim, H. W. Roesky, *Chem. Commun.* **2019**, *55*, 1359; b) A. Schulz, *Dalton Trans.* **2018**, *47*, 12827; c) B. Li, S. Kundu, A. C. Stückl, H. Zhu, H. Keil, R. Herbst-Irmer, D. Stalke, B. Schwederski, W. Kaim, D. M. Andrada, G. Frenking, H. W. Roesky, *Angew. Chem. Int. Ed.* **2017**, *56*, 397; *Angew. Chem.* **2017**, *129*, 407; d) N. Lichtenberger, R. J. Wilson, Armin R. Eulenstein, W. Massa, R. Clérac, F. Weigend, S. Dehnen, *J. Am. Chem. Soc.* **2016**, *138*, 9033; e) L. S. Konstantinova, I. E. Bobkova, Y. V. Nelyubina, E. A. Chulanova, I. G. Irtegova, N. V. Vasilieva, P. S. Camacho, S. E. Ashbrook, G. Hua, A. M. Z. Slawin, J. D. Woollins, A. V. Zibarev, O. A. Rakitin, *Eur. J. Org. Chem.* **2016**, 5585; f) A. Brückner, A. Hinz, J. B. Priebe, A. Schulz, A. Villinger, *Angew. Chem. Int. Ed.* **2015**, *54*, 7426; *Angew. Chem.* **2015**, *127*, 7534; g) P. Bissinger, H. Braunschweig, A. Damme, I. Krummenacher, A. K. Phukan, K. Radacki, S. Sugawara, *Angew. Chem. Int. Ed.* **2014**, *53*, 7360; *Angew. Chem.* **2014**, *126*, 7488; h) H. Fischer, *Landolt-Börnstein—Group II Molecules and Radicals, Numerical Data and Functional Relationships in Science and Technology, 26E1*, Springer, Berlin, **2008**; i) J. M. Rawson, A. Alberola, A. Whalley, *J. Mater. Chem.* **2006**, *16*, 2560; j) I. Krossing, J. Passmore, *Inorg. Chem.* **2004**, *43*, 1000; k) S. Loss, A. Magistrato, L. Cataldo, S. Hoffmann, M. Geoffroy, U. Röthlisberger, H. Grützmacher, *Angew. Chem. Int. Ed.* **2001**, *40*, 723; *Angew. Chem.* **2001**, *113*, 749; l) R. Fleischer, D. Stalke, *Coord. Chem. Rev.* **1998**, *176*, 431.

[3] R. Fleischer, S. Freitag, D. Stalke, *J. Chem. Soc. Dalton Trans.* **1998**, 193.

[4] S. V. Klementyeva, N. P. Gritsan, M. M. Khusniyarov, A. Witt, A. A. Dmitriev, E. A. Suturina, N. D. D. Hill, T. L. Roemmele, M. T. Gamer, R. T. Boeré, P. W. Roesky, A. V. Zibarev, S. N. Konchenko, *Chem. Eur. J.* **2017**, *23*, 1278.

[5] A. Armstrong, T. Chivers, M. Parvez, G. Schatte, R. T. Boeré, *Inorg. Chem.* **2004**, *43*, 3453.

[6] J. K. Brask, T. Chivers, B. McGarvey, G. Schatte, R. Sung, R. T. Boeré, *Inorg. Chem.* **1998**, *37*, 4633.

[7] a) K. Bestari, R. T. Oakley, A. W. Cordes, *Can. J. Chem.* **1991**, *69*, 94; b) G. Brands, A. Golloch, *Z. Naturforsch.* **1982**, *37b*, 1137; c) J. A. Hunter, B. King, W. E. Lindsell, M. A. Neish, *J. Chem. Soc. Dalton Trans.* **1980**, 880.

[8] R. Fleischer, S. Freitag, F. Pauer, D. Stalke, *Angew. Chem. Int. Ed. Engl.* **1996**, *35*, 204; *Angew. Chem.* **1996**, *108*, 208.

[9] H. M. Tuononen, T. Chivers, A. Armstrong, C. Fedorchuk, R. T. Boeré, *J. Organomet. Chem.* **2007**, *692*, 2705.

[10] T. Chivers, M. Parvez, G. Schatte, *Inorg. Chem.* **1996**, *35*, 4094.

[11] A. Armstrong, T. Chivers, M. Parvez, R. T. Boeré, *Angew. Chem. Int. Ed.* **2004**, *43*, 502; *Angew. Chem.* **2004**, *116*, 508.

[12] a) T. Kottke, D. Stalke, *J. Appl. Crystallogr.* **1993**, *26*, 615; b) D. Stalke, *Chem. Soc. Rev.* **1998**, *27*, 171; c) Bruker AXS Inc., *SAINT*, Madison, **2016**; d) L. Krause, R. Herbst-Irmer, G. M. Sheldrick, D. Stalke, *J. Appl. Crystallogr.* **2015**, *48*, 3; e) G. M. Sheldrick, *Acta Crystallogr. Sect. C* **2015**, *71*, 3; f) G. M. Sheldrick, *Acta Crystallogr. Sect. A* **2015**, *71*, 3; g) C. B. Hübschle, G. M. Sheldrick, B. Dittrich, *J. Appl. Crystallogr.* **2011**, *44*, 1281; h) A. Thorn, B. Dittrich, G. M.

Sheldrick, *Acta Crystallogr. Sect. A* **2012**, *68*, 448; i) M. Sevvana, M. Ruf, I. Usón, G. M. Sheldrick, R. Herbst-Irmer, *Acta Crystallogr. Sect. D* **2019**, *75*, 1040.

[13] M_3AsS_3 with A = Li: a) S. Huber, C. Preitschaft, R. Weihrich, A. Pfitzner, *Z. Anorg. Allg. Chem.* **2012**, *638*, 2542; b) D.-Y. Seung, P. Gravereau, L. Trut, A. Levasseur, *Acta Crystallogr. Sect. C* **1998**, *54*, 900; M = Na: c) P. M. Palazzi, *Acta Crystallogr. Sect. B* **1976**, *32*, 3175; M = K, Cu_2: d) J. E. Jerome, P. T. Wood, W. T. Pennington, J. W. Kolis, *Inorg. Chem.* **1994**, *33*, 1733.

[14] a) D. Leusser, J. Henn, N. Kocher, B. Engels, D. Stalke, *J. Am. Chem. Soc.* **2004**, *126*, 1781; b) J. Henn, D. Ilge, D. Leusser, D. Stalke, B. Engels, *J. Phys. Chem. A* **2004**, *108*, 9442.

[15] a) R. Fleischer, A. Rothenberger, D. Stalke, *Angew. Chem. Int. Ed. Engl.* **1997**, *36*, 1105; *Angew. Chem.* **1997**, *109*, 1140; b) J. Jung, A. Münch, R. Herbst-Irmer, D. Stalke, *Angew. Chem. Int. Ed.* **2021**, *60*, 5679; *Angew. Chem.* **2021**, *133*, 5742.

[16] D. Stalke, *Chem. Commun.* **2012**, *48*, 9559.

[17] S. Deuerlein, D. Leusser, U. Flierler, H. Ott, D. Stalke, *Organometallics* **2008**, *27*, 2306.

[18] a) E. R. de La Rie, A. Michelin, M. Ngako, E. Del Federico, C. Del Grosso, *Polym. Degrad. Stab.* **2017**, *144*, 43; b) E. Boros, M. J. Earle, M. A. Gîlea, A. Metlen, A.-V. Mudring, F. Rieger, A. J. Robertson, K. R. Seddon, A. A. Tomaszowska, L. Trusov, J. S. Vyle, *Chem. Commun.* **2010**, *46*, 716; c) T. Chivers, I. Drummond, *Inorg. Chem.* **1972**, *11*, 2525; d) B. S. Gorobets, A. A. Rogojine, *Luminescent spectra of minerals.* VIMS, Moscow, **2002**; e) D. Reinen, G.-G. Lindner, *Chem. Soc. Rev.* **1999**, *28*, 75.

[19] G. Selvaggio, A. Chizhik, R. Nißler, L. Kuhlemann, D. Meyer, L. Vuong, H. Preiß, N. Herrmann, F. A. Mann, Z. Lv, T. A. Oswald, A. Spreinat, L. Erpenbeck, J. Großhans, V. Karius, A. Janshoff, J. Pablo Giraldo, S. Kruss, *Nat. Commun.* **2020**, *11*, 1495.

[20] Deposition Numbers 2117636 (for **1_K@120 K**) and 2117635 (for **1_K@100 K**) contain the supplementary crystallographic data for this paper. These data are provided free of charge by the joint Cambridge Crystallographic Data Centre and Fachinformationszentrum Karlsruhe Access Structures service www.ccdc.cam.ac.uk/structures.

Manuscript received: November 5, 2021
Accepted manuscript online: December 14, 2021
Version of record online: January 14, 2022